Quantification of finite strain in the Pyrenean Slate Belt; a first assessment using $R_{\rm f}/\Phi$ method

Rien Corstanje^{1, 2}, Christoffel Klepper¹, Bart Rutgers¹, Igor J. van der Wal¹ & Bas van den Eeckhout¹

Department of Structural Geology, Geological Institute, University of Amsterdam, Nieuwe Prinsengracht
130, 1018 VZ Amsterdam, The Netherlands; ² present address: TNO-DGV, Institute of Applied Geoscience,
P.O. Box 285, 2600 AG Delft, The Netherlands

Received 27 December 1988; accepted in revised form 7 March 1989

Key words: Central Pyrenees, microconglomerates, R_f/Φ method, slate belt, strain analysis, suprastructure

Abstract

Strain analysis has been carried out on (micro)conglomeratic Cambro-Ordovician sediments from the Pallaresa area (Axial Zone of central Pyrenees). Twenty strain ellipsoids have been determined. After correction for refolding and faulting a bulk finite strain ellipsoid for the area was calculated. This ellipsoid has k-value 3.43 and low axial ratios (X/Y = 1.24, Y/Z = 1.07). The ellipsoid has a long axis (X) plunging steeply NE, an intermediate axis (Y) parallel to the gently WNW plunging mean fold axis of the area, and a nearly horizontal south plunging short axis (Z). The shortening direction (Z) is normal to the steep N-NNE dipping cleavage. During deformation the sediment pile in the area must have undergone vertical tectonic thickening by factor 1.15. It is argued that this value is a minimal estimate and inhomogenous deformation must be taken into account.

Introduction

The Variscan part of the Pyrenees contains a relatively large area which is occupied by upright folds. These folds affect lower Paleozoic siliciclastics, Silurian euxinic black slates. Devonian limestones and Carboniferous carbonates and clastics. Their attitude indicates N-S to NNE-SSW directed shortening, which has been fitted in the overall tectonic framework of the Variscan orogeny in western Europe by Matte (1986). The Variscan shortening direction (Z) thus appears well constrained. However, little is known about the orientation of the intermediate (Y) and long (X) axes of this Variscan deformational event in the Pyrenees. This poses the question whether the sediments have been thickened, and if so, to what extent. The answer is of relevance in order to understand parameters like thermal gradients and pressures during Pyrenean metamorphism. Furthermore, it is of importance with respect to a critical evaluation of tectonic scenarios forwarded in the literature. For example, thickening would hardly fit an extensional tectonic regime as suggested by Wickham & Oxburgh (1986). In addition, little thickening would be hard to explain in terms of a Himalayan type of orogeny (Matte, 1986).

From this point of view we have made an analysis of strain of the lower Paleozoic siliciclastics of the Pallaresa anticlinorium (Fig. 1).

Geological setting

Based on metamorphic and structural features, the Variscan part of the Pyrenees can be divided in two

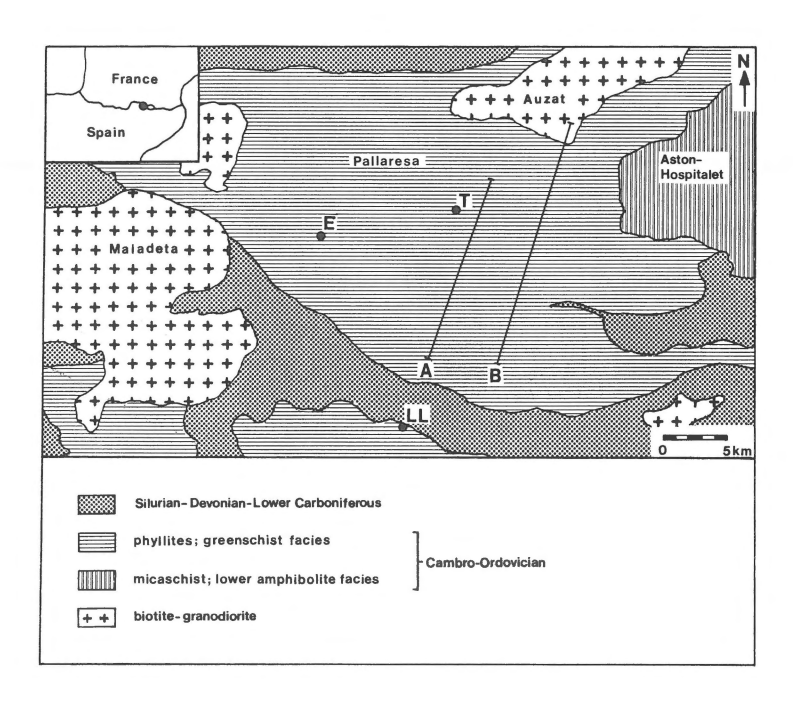


Fig. 1. Geological setting of the Pallaresa area (after Zwart, 1979). E – Esterri d'Aneu; LL – Llavorsi; T – Tabescan. A-B: lines of sections of Fig. 2.

domains:

- 1. an infrastructure with a high degree of metamorphism and usually flatlying structures (e.g. the Aston-Hospitalet massif in Fig. 1), and
- 2. an overlying suprastructure, with a much lower degree of metamorphism (lower greenstone facies) and steep to vertical structures (Zwart, 1979).

The investigated area, the Pallaresa anticlinorium, is situated in the suprastructure (Fig. 1). Structures and rock types have been studied by Zandvliet (1960), Hartevelt (1970), Losantos et al. (1986) and Laumonier & Guitard (1986).

The core of the Pallaresa anticlinorium exposes clastic sediments, predominantly slates and quartzites. These rocks are in general assumed to be of Cambro-Ordovician age. Laumonier (in press) proposes a Cambrian age. Interbedded in these rocks (micro)-conglomeratic horizons occur which we used for strain analysis. These conglomerates consist of up to 50 cm thick beds of well sorted, quartz pebbles. Pebble size is usually less than 1 cm. The rocks are usually clast supported, locally matrix supported.

Zandvliet (1960, p. 99) distinguished one phase of deformation, referred to as 'main phase' by Zwart (1979). Structures predating the main phase have been recognized west and south of the area (respectively Losantos et al., 1986; Speksnijder, 1986). The main phase resulted in the formation of large-scale open to tight upright folds with gently plunging axes. Structures trend E-W to ESE-WNW. Axial planar to these folds a well developed slaty cleavage is observed in pelitic beds. Cleavage is spaced or absent in psammitic layers. Macroscopically, flattening of pebbles parallel to the cleavage plane is observed. However, due to the massive nature of the rocks neither preferred orientation nor pebble shape can be deduced in the field.

Analytical methods

Structural analysis has been carried out in the field, which resulted in a general structural cross section (Fig. 2). In order to relate the results of our strain

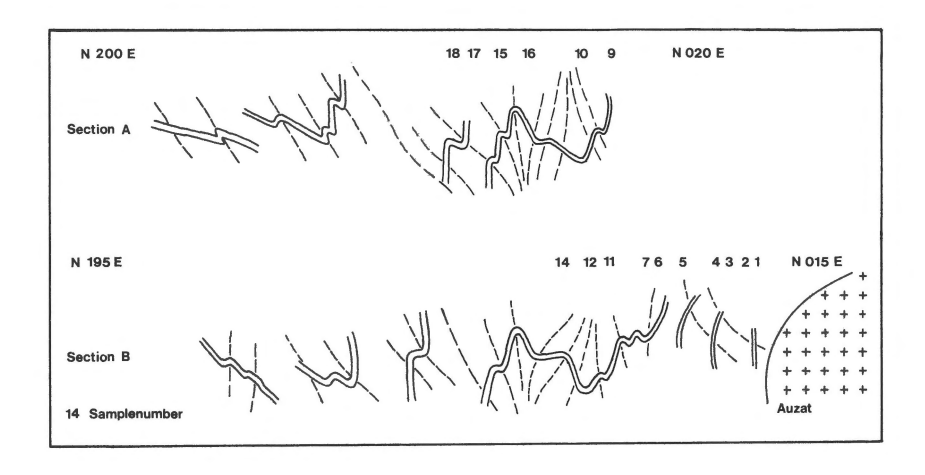


Fig. 2. Structural sections through the Pallaresa area. Section A: Vall Ribera de Cardos, Section B: Vall Ferrera. For location of the sections see Fig. 1. Sample numbers refer to Table 1.

analysis to the local geology oriented samples of the conglomerate beds were collected.

In the laboratory the samples were cut along three planes at large angles to each other. Such sections need not necessarily be orthogonal (Milton, 1980; Ramsay, 1967) nor parallel to the principal planes of the strain ellipsoid (Ramsay, 1967; Siddans, 1980). Each section has been photographed. From these photographs the axial ratio of each pebble cross section (R_f) was determined, and the orientation of the long axis of each pebble relative to a reference line (angle Φ) was measured. From these data a strain ellipse was determined for each section as described below. The three strain ellipses from each sample were subsequently used in computation of the strain ellipsoid.

The strain analysis in two dimensions has been carried out using two methods. The method of Shimamoto & Ikeda (1976) was used to define the angle between the reference line and the extension direction (X): R_f/Φ data of each pebble are expressed in matrix notation and from the final summation ellipse the X direction is determined by eigenvector analysis. The amount of strain was determined by Lisle's method (Lisle, 1977, 1985). Plots of pebble axial orientation (R_f/Φ) were compared with those predicted by homogeneous strain superimposed on an initially randomly sampled population whose original ellipses had their long

axes uniformly distributed. The amount of strain (R_s) is defined as the best fit of R_{i^-} and theta curves on the R_f/Φ diagram. R_{i^-} curves ('onion curves' Dunnet, 1969) are loci of constant initial shape, whereas theta-curves (Θ) are loci of constant initial orientation. To obtain valid results initial pebble orientation has to be random in the sample. Furthermore, pebbles have to deform homogeneously with the supporting matrix. An example of a R_f/Φ diagram with superimposed R_{i^-} and theta curves is shown in Fig. 3.

Theoretically an ellipsoid can be defined by, and may be reconstructed from any three non-parallel sections through it. In reality three strain ellipses, due to measurement errors and strain inhomogeneity, may not fit into one strain ellipsoid. The ellipses must first be adjusted to make them compatible, which is done by using the method of Milton (1980).

An adjustment ellipse is determined for each section by equalizing intersection lines of the ellipses on different sections. After multiplication of the adjustment ellipse with the original ellipse the three strain ellipses are compatible. Now, the strain ellipsoid may be determined by solving the three two-dimensional ellipse equations into a three-dimensional ellipsoid equation. The orientation and length of the principal axes of the ellipsoid are derived from the ellipsoid matrix by eigenvector analysis.

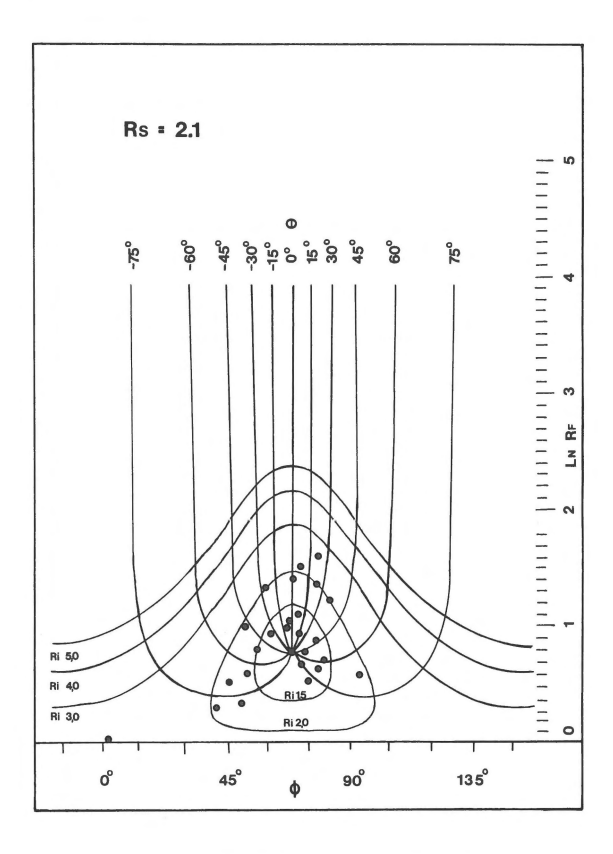


Fig. 3. Example of R_t/Φ diagram. The natural logarithm of the axial ratio of pebbles plotted against the angle of the longest axis with a reference line.

 R_s = strain value

R_i = initial axial ratio of pebble

R_f = axial ratio of pebble

 Θ = initial pebble orientation

 Φ = angle between X-direction of pebble and reference line

The Root-Mean-Square of the sum of residuals of the three adjustment ellipses can be regarded as an adjustment factor for the strain ellipsoid. This factor (which ranges from 0 to ∞) is an estimate for the degree of fit of the ellipsoid. Those ellipsoids of which the distortion factor exceeds 0.1 are excluded from the results (Table 1). We have chosen this value to exclude those ellipsoids whose size, shape and orientation probably is not representative for the original strain ellipsoid because of measurement errors.

Results

The results of the strain analysis are tabulated in Table 1, and are presented graphically in a Flinn-diagram and equal area stereonets (Figs. 4 and 5).

From the 20 analysed samples several yielded results unsuitable for further processing. Two categories can be distinguished:

- 1. strain ellipsoids with adjustment factors exceeding 0.1 as discussed above (samples 1, 2, 13, see Table 1), and
- 2. those ellipsoids whose XY planes deviate from the measured cleavage planes (samples 12, 12b, 19, see Table 1).

In the latter case the extension direction of the strain ellipsoid is more or less perpendicular to that shown by cleavage. Therefore this strain ellipsoid may not reflect the actual strain state. This may have been caused by measurement errors during sampling, or by a pre-deformation preferred orientation of the pebbles (e.g. by clast imbrication, or by earlier deformation), in which case the basic assumption for Lisle's method is not attained.

From the Flinn diagram two conclusions may be drawn:

- 1. there is a large variation in strain type, and
- 2. strain intensity is low.

Strain types in the area show a wide variety of k-values varying from flattening to constrictional deformation. Features like sorting of the conglomerate, clast-matrix ratio, pebble size, or local setting could, however, not be related to strain type.

Strain intensity in the area is surprisingly low considering the tight nature of folds and low angle between bedding and cleavage. Most X/Y and Y/Z values vary between 1.0 and 1.5. The mean strain ellipsoid for the area, determined from the cluster mean in the Flinn diagram, has low axial ratios (1.25) and a k-value of 1. This k-value indicates plane strain deformation since volume loss is of minor importance. Deformation by pressure solution (triangles in Fig. 4), however, causes marked deviations from the 'average' strain ratio. Pebbles truncated by cleavage planes indicate a solution perpendicular to the plane of maximum extension. Therefore the axial ratio of the pebbles, i.e. the strain intensity will be increased. Such variations in

Table 1. Finite strain ellipsoids for the Pallaresa area in the Central Pyrenees

Sample	Principal Axes	R	Adj.		Sample	Principal Axes	R	Adj.	
1 Wv 07	264/50 172/02 081/40	1.35 0.97 0.76	0.48 1.38	NU	11 Rt 09	151/68 254/05 347/21	1.30 0.94 0.82	0.09 2.53	
2 Wv 10	064/27 325/17 207/57	1.60 1.17 0.53	0.23 0.31	NU	12 Kch 107 (def)	222/16 130/06 022/73	1.41 1.05 0.68	0.10 0.63	NC
3 Wv 12	089/12 311/74 181/10	1.65 1.15 0.53	0.01 0.37	PS	12b Kch 107 (undef)	230/11 139/06 021/78	1.29 1.03 0.76	0.00 0.70	NC
4 Wv 14	015/61 110/03 202/29	1.53 1.34 0.49	0.10 <i>0.08</i>	PS	13 Kch 105	339/22 184/66 073/09	1.33 0.98 0.77	0.21 1.29	NU
5 Rt 07	097/48 349/15 247/38	1.33 0.90 0.83	0.05 5.23		14 CM 06A	043/56 208/33 302/07	1.41 1.05 0.68	0.05 0.17	
6 Rt 04	047/39 171/35 287/32	1.28 0.97 0.80	0.01 1.50		15 Rt 21B	028/63 271/13 175/23	1.11 1.04 0.87	0.05 0.37	
7 Rt 05	238/42 031/45 135/14	1.28 1.07 0.73	0.02 0.41		16 Rt 21	065/64 162/04 254/26	1.26 0.96 0.83	0.04 2.13	
8 Rt 02	250/12 129/68 344/19	1.16 0.97 0.88	0.02 2.02	UN	17 CM 04	345/59 231/14 134/27	1.20 1.07 0.78	0.00 0.32	
9 Wv 24	337/76 130/12 221/06	1.24 1.03 0.78	0.02 0.69		18 Rt 22B	258/12 101/77 349/05	1.13 0.99 0.89	0.10 1.17	UN
10 Wv 27	038/58 264/24 164/21	1.43 0.87 0.81	0.01 9.01	PS	19 CM 08A	164/28 256/04 354/62	1.12 1.03 0.86	0.02 0.43	NC

R = length of principal axis, Adj = calculated adjustment factor, k = Flinn value for strain ellipsoid, NU = not used (Adj > 0.10), UN = undeformed, PS = pressure solution, NC = normal to cleavage. Sample numbers refer to the structural profiles in Fig. 2.

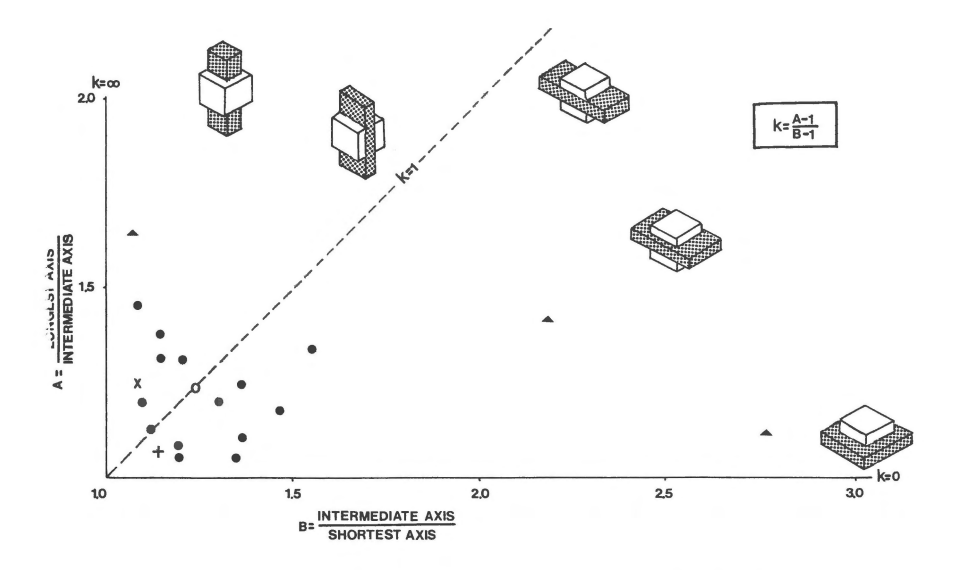


Fig. 4. Flinn diagram of microconglomerates from the Pallaresa area. Triangles refer to samples deformed by pressure solution. (+) and (\times) refer to bulk finite strain ellipsoids for the area respectively before and after rotation (see text for discussion). The cluster mean (\circ) of the Flinn diagram has been estimated after exclusion of samples deformed by pressure solution.

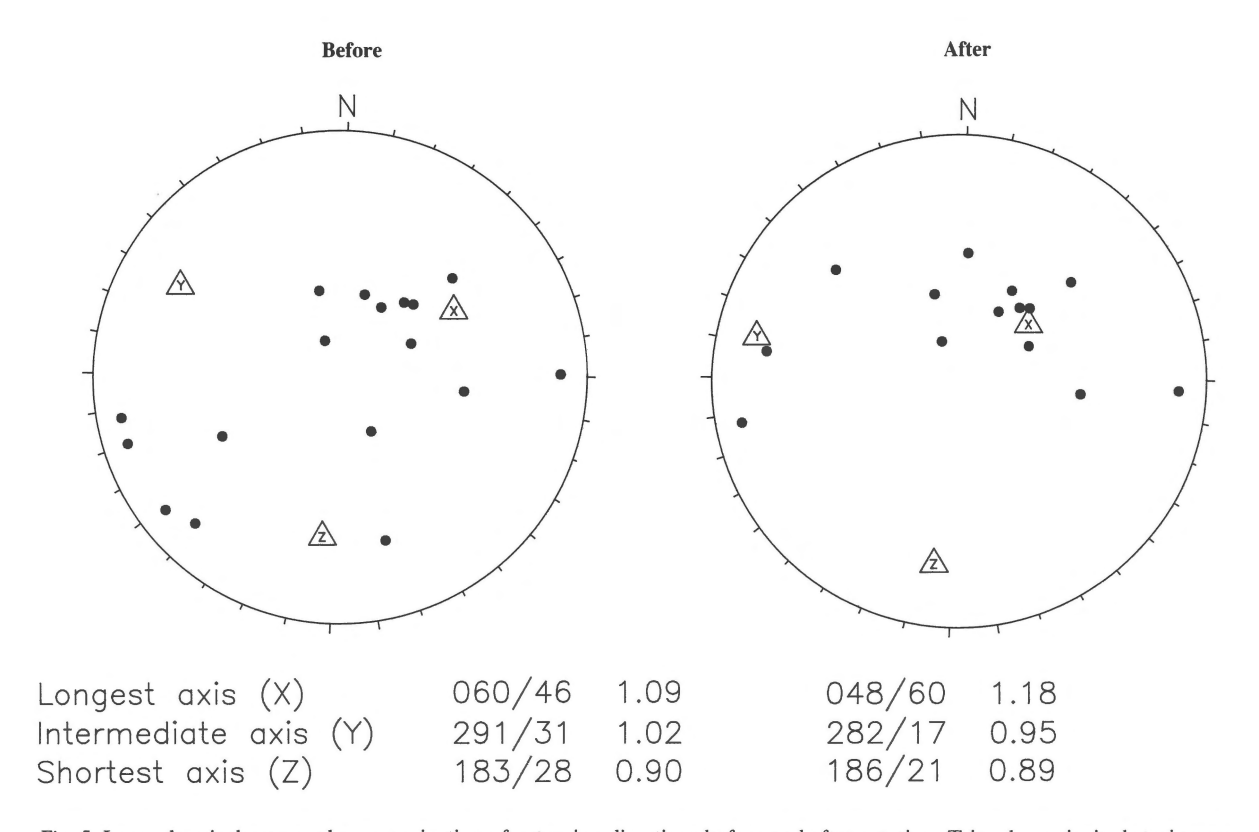


Fig. 5. Lower hemisphere equal-area projection of extension directions before and after rotation. Triangles: principal strain axes.

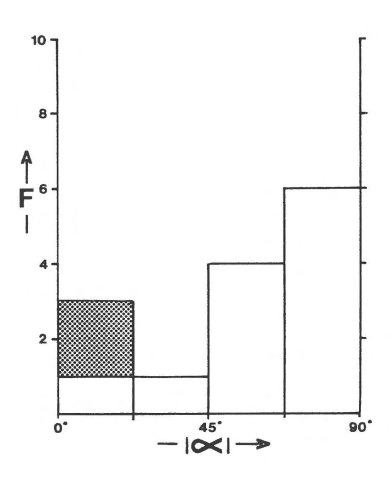


Fig. 6. Frequency distribution of absolute angles between extension direction and fold axis of the main phase (dashed samples are almost undeformed).

strain intensity are common in pressure solution aided deformation (Ramsay, 1967).

The equal area stereonet of Fig. 5a shows a good deal of scatter of principal extension directions. However, late disturbing effects have not been accounted for in this diagram. Such effects comprise cleavage fanning and block rotation due to faulting. As a consequence the diagram does not allow comparison of samples with respect to the relationship between strain ellipsoid and structural elements. To gain insight into this relationship, the orientation data from the samples were rotated so as to give the cleavage a common orientation of 010/70 and a fold axis plunging 280/15 (Fig. 7). The result of this manipulation is shown in Fig. 5b. It shows X-directions which deviate only a minor amount from the cleavage plane (XY). Furthermore, clustering of X-directions at a high angle to the fold axis is evident from this diagram.

The relationship between the structural elements and strain ellipsoid on a regional scale is brought out by Fig. 6. Some samples have their X-axes parallel to the fold axis. These samples (8, 18, see Table 1) show a very low strain intensity. The other samples show a normal frequency distribution around a steep plunging X-direction which is normal to the fold axis of the main phase.

The method of Shimamoto & Ikeda (1976) can

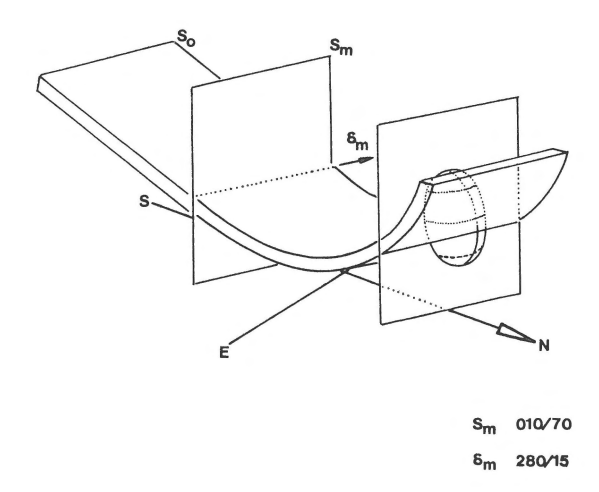


Fig. 7. Idealized fold and its calculated strain type for the Pallaresa area. The attitude of the fold represents the mean orientation of cleavage planes and fold axes as established during field work and by Zandvliet (1960).

be used to calculate a bulk finite strain ellipsoid for the area. The orientations and lengths of the principal strain axes may be calculated by means of eigenvalue analysis of the summation ellipsoid matrix. The orientation of the bulk finite strain ellipsoid for the area in Fig. 5a shows remarkable resemblance to the bulk finite strain ellipsoid in Fig. 5b in which cleavage fanning and block faulting is accounted for.

The mean strain ellipsoid for the area indicates a constrictional deformation type (k = 3.43) with a steep NE plunging X-direction and an XY-plane almost parallel to the cleavage (Figs. 7, 8).

Discussion

Two different aspects emerge from our results. First, deformation is low and shows considerable scatter of k-values and X-directions. Second, after correction for structural disturbances the attitude of most strain ellipsoids is remarkably similar.

The low degree of deformation, as evident from the bulk finite strain ellipsoid and the cluster mean in the Flinn diagram contrasts with the tight folds and low angle between bedding and cleavage observed in the field. In our opinion this indicates that deformation of the competent quartzite and con-

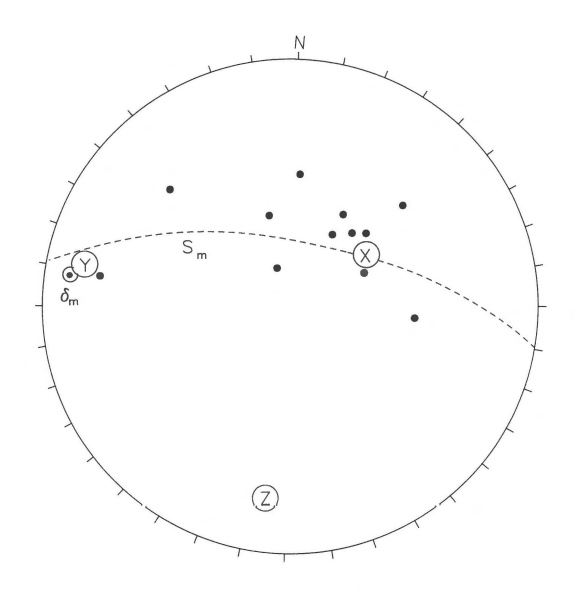


Fig. 8. Lower hemisphere equal-area projection of the bulk finite strain ellipsoid axes, fold axis and cleavage of the idealized main phase fold. Solid dots: X-axes of strain ellipsoids after manipulation; X, Y, Z: mean longest, intermediate and shortest strain axes; δ_M : fold axis; S_M : cleavage.

glomerate beds mainly has been accommodated by (buckle) folding and accompanying rotation and flexural slip, whereas interbedded pelitic beds have been deformed more intensely. Homogeneous deformation of competent beds probably was of minor importance. Consequently, with Borradaile (1981) we consider the estimated bulk finite strain as a minimal one.

The Flinn diagram shows considerable scatter of k-values. Features like pebble size, distribution of pebbles and matrix, and sorting of the conglomerate could not be related to a specific strain type. Neither could it be shown that this distribution of the diagram is due to the presence of zones or areas with different deformation type or history. We consider the scatter as an original effect, which corroborates the concept of heterogeneous deformation.

Comparison of corrected strain ellipsoids (Figs. 5b, 8) shows remarkable clustering of X-axis directions. The orientation of the X-axis suggests vertical thickening, more or less perpendicular to the fold axis during main phase deformation of the area. In this respect it is important to consider the

orientation of the structural elements during Variscan deformation. Like Zwart (1979) we favour the hypothesis that the attitude of the main phase cleavage has been steep in these times. Assuming that the orientation of the fold of Fig. 7 represents its Variscan attitude, vertical thickening with factor 1.15 can be calculated from the strain ellipsoid.

Several authors have discussed the discrepancy between pressure during metamorphism and lithostatic load provided by the thickness of the stratigraphic column (Zwart, 1979; Van den Eeckhout, 1986). The latter author estimated 5 km of sediment to have been present, whereas pressure during metamorphism has been estimated at 2–3 kbar, or 7-10 km (in the Hospitalet massif). Folding of the sedimentary pile (suprastructure formation) predates metamorphism in the massifs of Aston and Hospitalet (Van den Eeckhout & Zwart, 1988). Thickening by a factor 1.15 during folding evidently is too low to explain pressures during metamorphism. However, bearing in mind that this value is a minimal one, we suggest that thickening of the stratigraphic pile during folding has contributed significantly to the increase of pressure.

The data presented in this paper should be regarded as a first assessment of the finite strain in the Pyrenean slate belt. We feel it is yet too early to interpret them in tectonic terms as mentioned in the Introduction. However, at present we tend to believe that the concluded thickening is hard to fit into the tectonic scenario proposed by Wickham & Oxburgh (1986), i.e. one that accounts for crustal stretching only.

Conclusions

Microconglomerates of the Pallaresa area reveal low strain and a wide variety of strain types, as determined by methods described by Lisle (1977), Shimamoto & Ikeda (1976) and Milton (1980). Strain types vary from flattening to constrictional which may be attributed to heterogeneous strain, and additionally to the fact that assumptions of analytical methods used may not have been valid, because of sedimentary or tectonic initial shapes and fabrics.

Orientations of the ellipsoids show large scatter, but when corrected for late deformations, scatter is significantly reduced. The resulting cluster allowed deduction of a bulk finite strain ellipsoid of a constrictional type (k=3.43). Its X-axis steeply plunges NE, its intermediate axis is parallel to the mean fold axis of the area and the major shortening direction plunges gently south, perpendicular to cleavage.

Thickening occurred during main phase folding of the area. Vertical tectonic thickening is in the order of 1.15, which is considered to be a minimal value.

Acknowledgements

We are sincerely grateful to Jan Diederik van Wees and Ronald van Balen for programming the statistical methods. Drs. Richard Lisle and John Savage are thanked for constructive review.

References

- Borradaile, G.J. 1981 Minimum strain estimate from conglomerates with ductility contrast J. Struct. Geol. 3: 295–297
- Dunnet, D. 1969 A technique of finite strain analysis using elliptical particles Tectonophysics 7: 117–136
- Hartevelt, J.J.A. 1970 Geology of the Upper Segre and Valira valleys, Central Pyrenees, Andorra/Spain Leidse Geologische Mededelingen 45: 167–236
- Laumonier, B. & G. Guitard 1986 Lower Paleozoic of the Pyrenean Axial Zone, a synthesis – C.R. Acad. Sc. Paris 302: 473–478
- Laumonier, B. (in press) Les groupes de Canaveilles et de Jujols

- ('Paleozoic Inférieur') des Pyrénées Orientales. Arguments en faveur de l'âge essentiellement Cambriens de ces séries – Hercynica
- Lisle, R.J. 1977 Clastic grain shape in relation to cleavage from the Aberystwyth Grits, Wales – Tectonophysics 39: 381–395
- Lisle, R.J. 1985 Geological Strain Analysis Pergamon Press, Oxford: 99 pp
- Losantos, M., J. Palau & J. Sanz 1986 Considerations about Hercynian thrusting in the Marimaña massif (central Pyrenees) – Tectonophysics 129: 71–79
- Matte, Ph. 1986 Tectonics and plate tectonics model for the Variscan belt of Europe Tectonophysics 126: 329–374
- Milton, N.J. 1980 Determination of the strain ellipsoid from measurements on any three sections – Tectonophysics 64: T19–T27
- Ramsay, J.G. 1967 Folding and fracturing of rocks McGraw-Hill, New York: 567 pp
- Shimamoto, T. & Y. Ikeda 1976 A simple algabraic method for strain estimation from deformed ellipsoidal objects, 1. Basic theory – Tectonophysics 36: 315–337
- Siddans, A.W.B. 1980 Analysis of three dimensional, homogeneous finite strain using ellipsoidal objects Tectonophysics 64: 19–27
- Speksnijder, A. 1986 Geological analysis of Paleozoic largescale faulting in the south-central Pyrenees – Thesis, State Univ. Utrecht, Geologica Ultraiectina 43: 1–211
- Van den Eeckhout, B. 1986 A case study of a mantled gneiss antiform, the Hospitalet massif, Pyrenees (Andorra, France)
 Thesis, State Univ. Utrecht, Geologica Ultraiectina, 45: 1–193
- Van den Eeckhout, B. & H.J. Zwart 1988 Hercynian crustalscale shear zone in the Pyrenees – Geology 16: 135–138
- Wickham, S.M. & E.R. Oxburgh 1986 A rifted tectonic setting for Hercynian high-thermal gradient metamorphism in the Pyrenees – Tectonophysics 129: 53–70
- Zandvliet, J. 1960 The geology of the Upper Salat and Pallaresa valleys, central Pyrenees, France/Spain Leidse Geologische Mededelingen 25: 1–127
- Zwart, H.J. 1979 The geology of the Central Pyrenees Leidse Geologische Mededelingen 50: 1–74